

## Seismic performance of reinforced engineered cementitious composite shear walls

Mo Li<sup>a</sup>, Hieu C. Luu<sup>b</sup>, Chang Wu<sup>c</sup>, Y.L.Mo<sup>\*d</sup> and Thomas T.C. Hsu<sup>e</sup>

*Department of Civil & Environmental Engineering, University of Houston, Houston, Texas 77204-4003, United States*

*(Received October 11, 2013, Revised July 30, 2014, Accepted October 8, 2014)*

**Abstract.** Reinforced concrete (RC) shear walls are commonly used for building structures to resist seismic loading. While the RC shear walls can have a high load-carrying capacity, they tend to fail in a brittle mode under shear, accompanied by forming large diagonal cracks and bond splitting between concrete and steel reinforcement. Improving seismic performance of shear walls has remained a challenge for researchers all over the world. Engineered Cementitious Composite (ECC), featuring incredible ductility under tension, can be a promising material to replace concrete in shear walls with improved performance. Currently, the application of ECC to large structures is limited due to the lack of the proper constitutive models especially under shear. In this paper, a new Cyclic Softening Membrane Model for reinforced ECC is proposed. The model was built upon the Cyclic Softening Membrane Model for reinforced concrete by (Hsu and Mo 2010). The model was then implemented in the OpenSees program to perform analysis on several cases of shear walls under seismic loading. The seismic response of reinforced ECC compared with RC shear walls under monotonic and cyclic loading, their difference in pinching effect and energy dissipation capacity were studied. The modeling results revealed that reinforced ECC shear walls can have superior seismic performance to traditional RC shear walls.

**Keywords:** constitutive model; engineered cementitious composite, shear walls, nonlinear finite element, pinching effect

### 1. Introduction

Under earthquakes, structures are usually damaged because of inadequate earthquake resistance such as low quality materials, poor workmanship and improper selection of the structural system (Yön *et al.* 2013). There is a common belief that shear walls are essential structural components to improve the safety and serviceability of buildings subjected to earthquake. Most of shear walls used in structures are made of reinforced concrete (RC). The damages reported from recent

---

\*Corresponding author, Professor, E-mail: [yomo@uh.edu](mailto:yomo@uh.edu)

<sup>a</sup>Assistant Professor, E-mail: [moli@uh.edu](mailto:moli@uh.edu)

<sup>b</sup>Ph.D. Student, E-mail: [hclu@uh.edu](mailto:hclu@uh.edu)

<sup>c</sup>Ph.D. Student, E-mail: [trangwu27@gmail.com](mailto:trangwu27@gmail.com)

<sup>d</sup>Professor, E-mail: [yomo@uh.edu](mailto:yomo@uh.edu)

<sup>e</sup>Moores Professor, E-mail: [thsu@uh.edu](mailto:thsu@uh.edu)

earthquakes showed that RC shear walls are not always effective in protecting structures from serious damage when earthquakes happen (Ozmen *et al.* 2013). The reasons why RC shear walls failed are that they are basically governed by shear, accompanied by forming large diagonal cracks, bond splitting between concrete and steel reinforcement, and spalling of the concrete cover (Zhong 2005). In addition, the shear capacity of RC walls depends strongly on the softening of concrete struts in the principal compression direction due to the principal tension in the perpendicular direction (Hsu and Mo 2010). Therefore, a study of how to improve the seismic behavior of shear walls is urgently significant.

The brittle failure mode of RC shear walls can be fundamentally attributed to the brittle nature of concrete material. In order to improve the shear capacity, ductility and energy dissipation capacity of RC shear walls, one approach is to replace brittle concrete by a ductile cementitious material such as Engineered Cementitious Composite (ECC)(Li 1994). ECC represents a family of high performance fiber-reinforced cementitious composite materials that uniquely feature tensile ductility and intrinsic crack width control capacity with a moderate amount (2% by volume) of short discontinuous fibers such as polyethylene, poly-vinyl alcohol or polypropylene fibers(Li 1993, Li *et al.* 2002). While containing similar ingredients as concrete or Fiber Reinforced Concrete (FRC), the microstructure of ECC can be deliberately tailored through the use of micromechanical models to achieve tensile strain-hardening behavior and ductility levels approximately 200 to 600 times that of concrete under tension, thereby leading to delayed fracture localization (Fig.1) (Li 2002, Li and Li 2009, Li and Li 2012). The fiber/matrix interfacial micromechanical parameters are strategically tailored to allow ECC to dissipate energy through multiple microcracking with crack widths less than 100  $\mu\text{m}$ . The tensile strain-hardening behavior of ECC significantly differentiates it from other FRCs such as steel, polymeric, glass, and carbon fiber reinforced concretes that exhibit tension-softening behavior. While ECC has been shown as a promising material for seismic applications (Kanda *et al.* 1998, Parra-Montesinos and Wight 2000, Fischer and Li 2002, Kesner and Billington 2002, Fischer and Li 2003), its wide adoption in large structures desires proper constitutive models that can account for both monotonic and cyclic loading especially under shear.

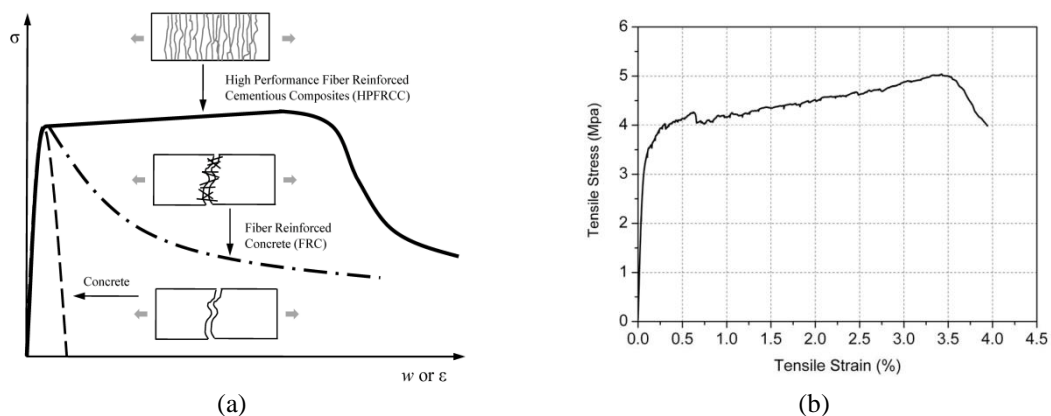


Fig. 1(a) Uniaxial tensile stress  $\sigma$  vs. strain  $\epsilon$  or (crack opening  $w$ ) constitutive relation of concrete, FRC, and ECC; (b) a typical experimental curve of ECC under uniaxial tension

Over the past two decades, a significant amount of research in developing constitutive models of reinforced concrete has been performed at the University of Houston. The cyclic softening membrane model (CSMM) developed by Mansour *et al.* (2005) is the most recent model to predict shear behavior of RC structural panels under cyclic shear loading. Zhong (2005) implemented the model into a finite element program called SCS using OpenSees as a frame work. The SCS has an excellent capability to predict behavior of a series of shear walls experimentally tested by Gao (Zhong 2005). In this paper, the CSMM based finite element program was modified to account for the unique properties of ECC, especially its ductility under tension. The seismic performance of reinforced ECC shear walls was then numerically studied. Parametric studies were conducted to investigate the effect of varied tensile and compressive parameters, as well as pinching characteristics on the seismic performance of reinforced ECC shear walls. As ECC is a family of cementitious materials that can be deliberately tailored based on micromechanical models to possess different material properties dictated by specific structural requirements, the parametric finite element analyses will provide profound insights on how the material ductility can be translated into structural load carrying capacity, and how to further optimize the ECC material for the maximized seismic performance of shear walls.

## 2. Cyclic softening membrane model (CSMM)

This paper aims at expanding the scope of the CSMM model for RC to account for the different properties of ECC. In order to develop the so-called CSMM-ECC model, the basic principles of the CSMM model for RC is summarized first.

### 2.1 Formulation of CSMM

#### 2.1.1 Coordinate systems in CSMM

Three Cartesian coordinates,  $x$ - $y$ , 1-2 and  $x_{si}$ - $y_{si}$ , are defined in the reinforced concrete elements, as demonstrated in Fig. 2. Coordinate  $x$ - $y$  defines the local coordinate of the elements. Coordinate 1-2 represents the principal stress directions of the applied stresses that has an angle  $\theta_1$  with respect to the  $x$ -axis. Steel bars can be oriented in different directions in the elements. Coordinate  $x_{si}$ - $y_{si}$  indicates the direction of the ‘ $i^{\text{th}}$ ’ group of rebars, where the ‘ $i^{\text{th}}$ ’ group of rebars are located in the direction of axis  $x_{si}$  with an angle  $\theta_{si}$  to the  $x$ -axis. The stress and strain vectors in  $x$ - $y$  coordinates and 1-2 coordinates are denoted as  $[\sigma_x, \sigma_y, \tau_{xy}]^T$ ,  $[\varepsilon_x, \varepsilon_y, 0.5\gamma_{xy}]^T$ ,  $[\sigma_1, \sigma_2, \tau_{12}]^T$  and  $[\varepsilon_1, \varepsilon_2, 0.5\gamma_{12}]^T$ , respectively.

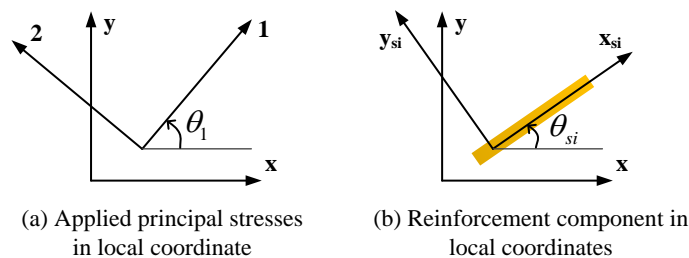


Fig. 2 Three cartesian coordinate systems

### 2.1.2 Equilibrium and compatibility equations

The applied stresses in the  $x$ - $y$  coordinate ( $\sigma_x$ ,  $\sigma_y$  and  $\tau_{xy}$ ) are related to the internal concrete stresses ( $\sigma_x^c$ ,  $\sigma_y^c$  and  $\tau_{xy}^c$ ) in the principal stress directions, and the steel bar stresses ( $f_{si}$ ) in the bar directions by the following equilibrium equation:

$$\begin{Bmatrix} \sigma_x \\ \sigma_y \\ \tau_{xy} \end{Bmatrix} = [T(-\theta_1)] \begin{Bmatrix} \sigma_1^c \\ \sigma_2^c \\ \tau_{12}^c \end{Bmatrix} + \sum_i [T(-\theta_{si})] \begin{Bmatrix} \rho_{si} f_{si} \\ 0 \\ 0 \end{Bmatrix} \quad (1)$$

Where  $\rho_{si}$  is the steel ratio in the  $i^{\text{th}}$  direction;  $[T(-\theta_1)]$  and  $[T(-\theta_{si})]$  are the transformation matrices from the 1-2 coordinate and the  $x_{si}$ - $y_{si}$  coordinate to the  $x$ - $y$  coordinate, respectively.

The relationships between the biaxial steel strains ( $\varepsilon_{si}$ ) in the  $x_{si}$ - $y_{si}$  coordinate and the biaxial concrete strains ( $\varepsilon_1$  and  $\varepsilon_2$ ) in the 1-2 coordinate are derived by the following compatibility equation:

$$\begin{Bmatrix} \varepsilon_{si} \\ \varepsilon_{s'i} \\ 0.5\gamma_{si} \end{Bmatrix} = [T(\theta_{si} - \theta_1)] \begin{Bmatrix} \varepsilon_1 \\ \varepsilon_2 \\ 0.5\gamma_{12} \end{Bmatrix} \quad (2)$$

### 2.1.3 Uniaxial strain and biaxial strain

In reality, uniaxial tests are usually performed in laboratory to determine material properties. In order to solve problems in 2-D dimension, the biaxial strains need to be converted to uniaxial strains so that the uniaxial constitutive material model tested in laboratory can be used. The uniaxial strains are related to the biaxial strains by the Poisson Ratios of cracked concrete.

$$\begin{Bmatrix} \bar{\varepsilon}_1 \\ \bar{\varepsilon}_2 \\ 0.5\gamma_{12} \end{Bmatrix} = [V] \begin{Bmatrix} \varepsilon_1 \\ \varepsilon_2 \\ 0.5\gamma_{12} \end{Bmatrix}; [V] = \begin{bmatrix} 1 & \nu_{12} & 0 \\ 1 - \nu_{12}\nu_{21} & 1 - \nu_{12}\nu_{21} & 0 \\ \nu_{21} & 1 & 0 \\ 1 - \nu_{12}\nu_{21} & 1 - \nu_{12}\nu_{21} & 0 \\ 0 & 0 & 1 \end{bmatrix} \quad (3)$$

In Eq. (3),  $\nu_{12}$  is the ratio of the resulting tensile strain increment in the principal 1 direction to the source compressive strain increment in the principal 2 direction, and  $\nu_{21}$  is the ratio of the resulting compressive strain increment in the principal 2 direction to the source tensile strain increment in the principal 1 direction. Values for  $\nu_{12}$  and  $\nu_{21}$  for reinforced concrete elements were derived from the panel tests by Zhu and Hsu (2002).

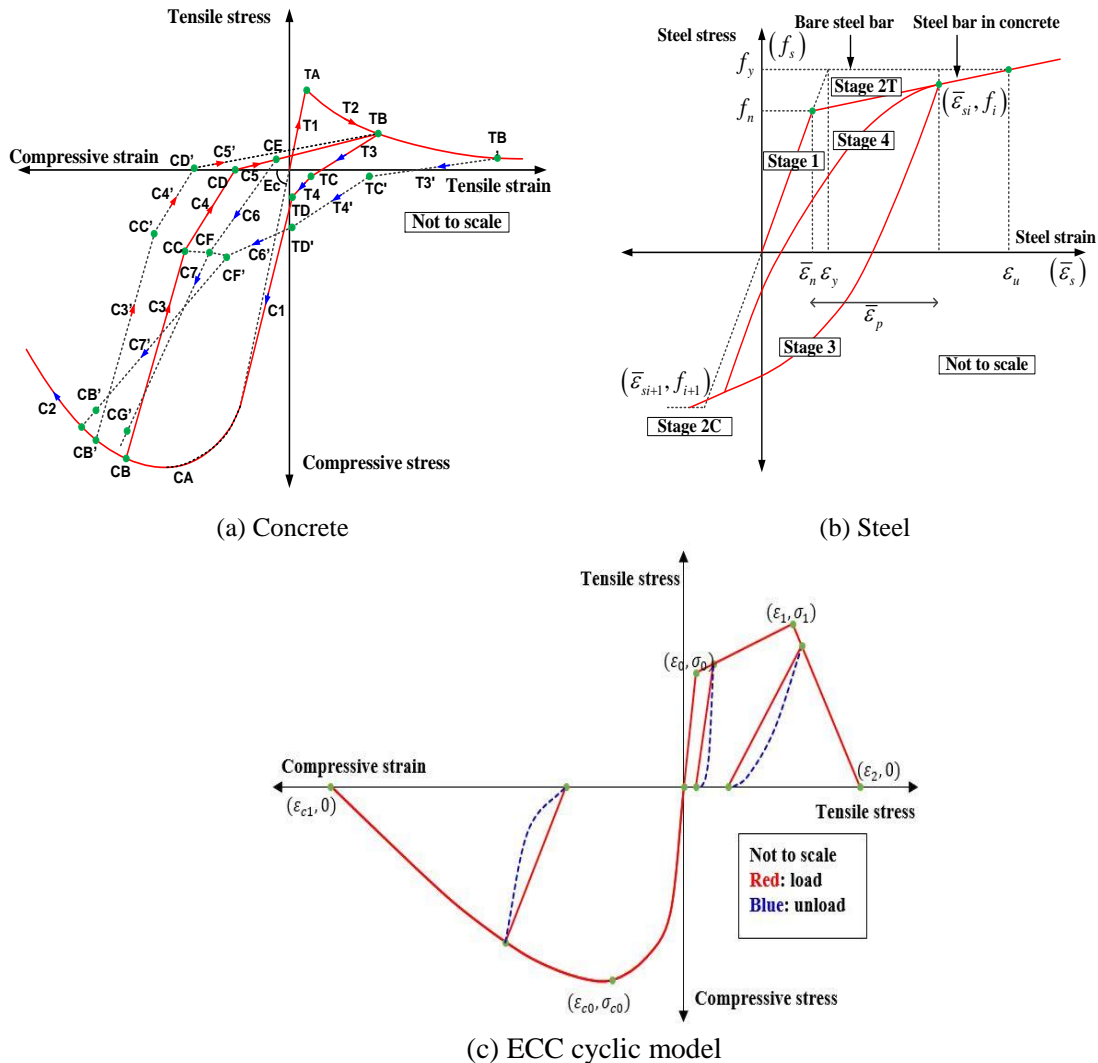


Fig. 3 Cyclic stress-strain relationships of materials.

2.1.4 Uniaxial constitutive model for concrete and embedded steel

The cyclic uniaxial constitutive relationships of concrete with embedded mild steel bars were proposed by Mansour (2001). The characteristics of these concrete constitutive laws include: (1) the softening effect on the concrete in compression due to the tensile strain in the perpendicular direction; (2) the softening effect on the concrete in compression under reversed cyclic loading; (3) the opening and closing of cracks, which are taken into account in the unloading and reloading stages, as shown in Fig 3a. The smeared yield stress of embedded mild steel bars is lower than the yield stress of bare steel bars and the hardening ratio of steel bars after yielding is calculated from the steel ratio, steel strength and concrete strength. The unloading and reloading stress-strain curves of embedded steel bars take into account the Bauschinger effect, as shown in Fig. 3b. Fig. 3c indicates the reversed cyclic model for ECC.

### 2.1.5 Finite element implementation

The constitutive laws discussed previously are combined with the equilibrium and compatibility equations to form a tangential constitutive matrix  $[D]$  for an element. The detailed derivation of the matrix  $[D]$  is presented in Zhong (2005). The formulation to determine  $[D]$  is given as follows:

$$[D] = \partial \begin{Bmatrix} \sigma_x \\ \sigma_y \\ \tau_{xy} \end{Bmatrix} / \partial \begin{Bmatrix} \varepsilon_x \\ \varepsilon_y \\ 0.5\gamma_{xy} \end{Bmatrix} \quad (4)$$

$[D]$  is evaluated by:

$$[D] = [T(-\theta_1)][D_c][V][T(\theta_1)] + \sum_i [T(-\theta_{si})][D_{si}][T(\theta_{si} - \theta_1)][V][T(\theta_1)] \quad (5)$$

In Eq. (5),  $[V]$  is the matrix defined in Eq. (3) which translates the biaxial strains into uniaxial strains using the Hsu/Zhu ratios.  $[D_c]$  and  $[D_{si}]$  are the uniaxial tangential constitutive matrix of concrete and the uniaxial tangential constitutive matrix of steel, respectively.  $[D_c]$  and  $[D_{si}]$  are determined as follows:

$$[D_c] = \begin{bmatrix} \bar{E}_1^c & \frac{\partial \sigma_1^c}{\partial \bar{\varepsilon}_2} & 0 \\ \frac{\partial \sigma_2^c}{\partial \bar{\varepsilon}_1} & \bar{E}_2^c & 0 \\ 0 & 0 & G_{12}^c \end{bmatrix}; [D_{si}] = \begin{bmatrix} \rho_{si} \bar{E}_{si} & 0 & 0 \\ 0 & 0 & 0 \\ 0 & 0 & 0 \end{bmatrix} \quad (6)$$

In Eq. (6),  $\bar{E}_1^c$ ,  $\bar{E}_2^c$  and  $\bar{E}_{si}$  are the tangential stiffness of uniaxial moduli of concrete and reinforcement which are computed at a stress/strain state. The derivatives of stress over strain  $\partial \sigma_1^c / \partial \bar{\varepsilon}_2$  and  $\partial \sigma_2^c / \partial \bar{\varepsilon}_1$  can be obtained by using the uniaxial constitutive relationships and taking into account the states of the concrete stresses and uniaxial strains in the 1-2 directions (Zhong 2005).  $G_{12}^c$  is the shear modulus of concrete and is evaluated by the following equation.

$$G_{12}^c = \frac{\sigma_1^c - \sigma_2^c}{\varepsilon_1 - \varepsilon_2} \quad (7)$$

## 2.2 Program SCS and Validation

### 2.2.1 Implementation

OpenSees stands for Open System for Earthquake Engineering Simulation (OpenSees 2013). OpenSees has been developed in the Pacific Earthquake Engineering Center (PEER) and is an object-oriented framework for simulation applications in earthquake engineering using finite element methods. An object-oriented framework is a set of cooperating classes that can be used to generate software for a specific class of problem, such as finite element analysis. The framework dictates overall program structure by defining the abstract classes, their responsibilities, and how

these classes interact. OpenSees is a communication mechanism for exchanging and building upon research accomplishments, and has the potential for a community code for earthquake engineering because it is an open source.

Using OpenSees as the finite element analysis framework, a nonlinear finite element program titled Simulation of Concrete Structures (SCS) was developed for the simulation of reinforced concrete structures subjected to monotonic and reversed cyclic loading (Mo *et al.* 2008). To create SCS program, the CSMM was implemented in OpenSees, three new material modules, namely SteelZ01, ConcreteZ01 and RCPlaneStress were developed. SteelZ01 and ConcreteZ01 are the uniaxial material modules, in which the uniaxial constitutive relationships of steel and concrete specified in the CSMM are defined, as shown in Fig. 3. The RCPlaneStress is implemented with the quadrilateral element to represent the four-node reinforced concrete membrane elements. The uniaxial materials of SteelZ01 and ConcreteZ01 are related with material RCPlaneStress to determine the material stiffness matrix of membrane reinforced concrete in RCPlaneStress.

### 2.2.2 Validation

Nine different framed shear walls were tested by Gao (1999) to evaluate the seismic performance of shear walls under constant axial load and reserved cyclic loading. In this article, two of these shear walls are selected for analysis. The wall dimensions are 914.4 mm by 914.4 mm with a thickness of 76.2 mm. The cross section of the boundary columns is 152.4 mm square. The details of the reinforcement of the specimen are illustrated in Fig. 4a. The bottom left and right corners of each specimen were supported by a hinge and a roller, respectively. Table 1 gives the material properties, reinforcement ratio and axial load ratio of each specimen. As noted from Table 1, the concrete strengths used in the two specimens are very close. Specimen SW13 has less reinforcement ratio and lower axial load ratio than Specimen SW4. As observed from the test results, Specimen SW13 has ductile behavior and Specimen SW4 has brittle behavior (Gao 1999).

Finite element analyses were conducted on the shear walls named SW4 and SW13. The two specimens were modeled by the finite element mesh, as illustrated in Fig. 4b. The wall panel are simulated by RCPlaneStress quadrilateral elements, mentioned above. The boundary columns and beams are simulated with NonlinearBeamColumn elements, which are available elements in

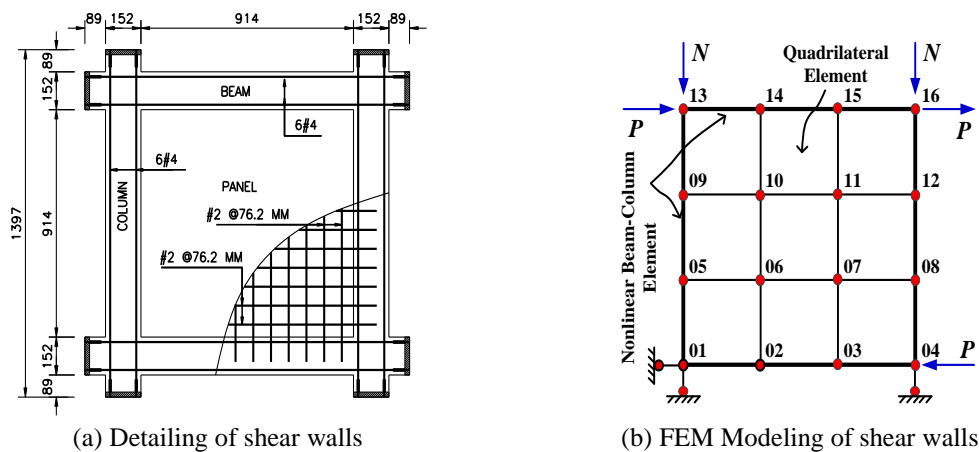


Fig. 4 Frame shear walls (Gao 1999)

Table 1 Dimensions and properties of specimens

Specimen name	$f'_c$ (MPa)	Column & Beam			Wall panel		Vertical Load	
		Hoop steel (mm)	Long. steel	Long. steel (%)	Panel steel (mm)	Panel steel (%)	P (kN)	P/Po Ratio
SW4	49.51	D3@63.5	6#4	3.33	#2@152.4	0.55	534	0.46
SW13	56.91	#2@63.5	6#4	3.33	W2@152.4	0.23	89	0.07

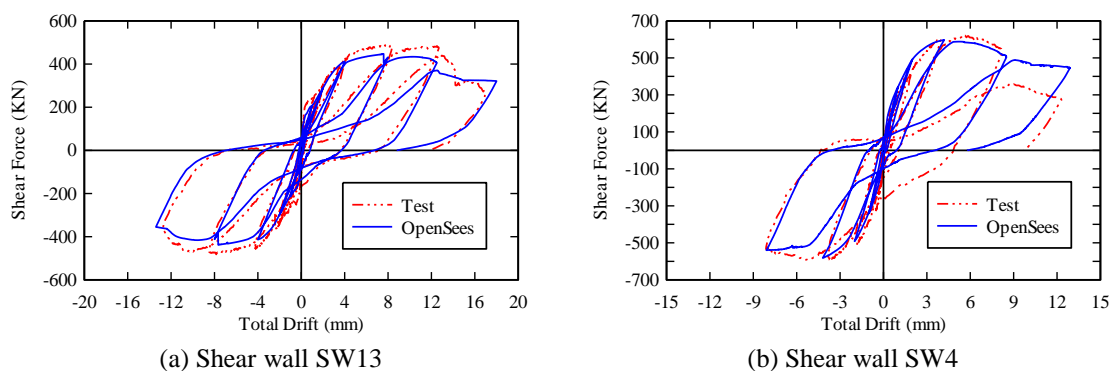


Fig. 5 Seismic behaviors of shear walls under cyclic loading.

OpenSees. The axial loads acting on the columns were applied as vertical nodal forces which remain constant in the analysis. The comparison of the analytical result with test data of the shear force-drift relationship of the structures is illustrated in Fig. 5. The analytical result is shown to provide a good correlation with experimental data. The primary backbone curve, the initial stiffness, the yield point, the peak strength, the descending branch, and the failure characteristics of the analytical results match very closely with the experimental data.

### 3. Constitutive models of ECC

To integrate ECC into the CSMM model, the constitutive laws of normal concrete in CSMM is modified to account for the unique characteristics of ECC. First, the tension-softening behavior of normal concrete is replaced by the tensile strain-hardening behavior of ECC, as shown in Fig. 6a. The tensile strain-hardening of ECC is simplified as a tri-linear model: (a) the first linear segment represents the elastic straining of the material until the first microcrack forms.  $f_{t1}$  denotes the first-cracking strength; (b) the second linear segment corresponds to the strain-hardening stage of ECC accompanied by sequentially forming multiple steady-state microcracks, until one of these microcracks exhausted its fiber-bridging capacity.  $f_{t2}$  denotes the ultimate tensile strength; (c) the third linear segment corresponds to the tension-softening stage of ECC, while the material behaves like regular FRC. During this stage, the final failure crack turns into a Griffith crack. The tensile stress drops as the crack opens. Second, the strain at maximum compression stress of ECC is modified to be higher than concrete, as shown in Fig. 6b. This is because the relatively lower Young's modulus of ECC. The reason for the lower Young's modulus of ECC is that ECC does not contain any coarse aggregates.

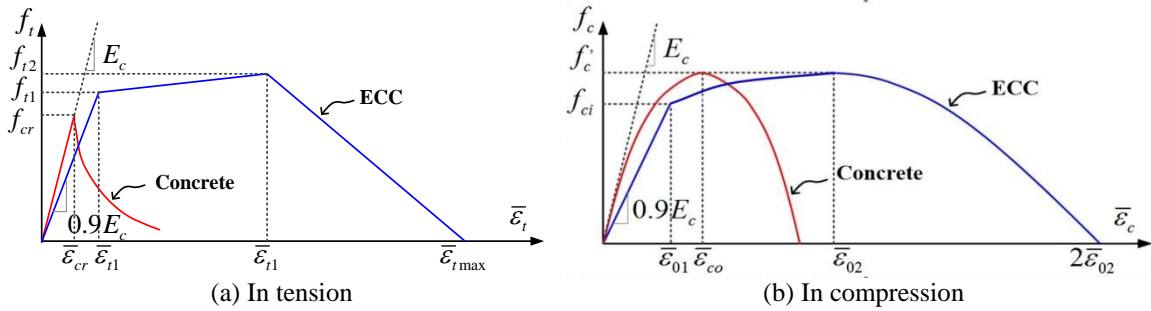


Fig. 6 Smearing uniaxial stress-strain relationships of concrete and ECC.

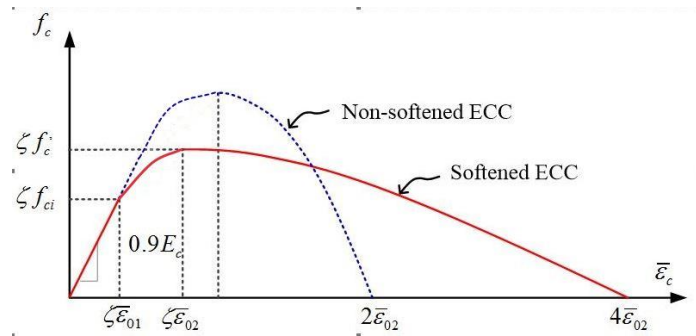


Fig. 2 Softening stress-strain relationship of ECC

Similar to concrete, the softening effect of ECC subjected to shear needs to be considered because the biaxial state of stress is different from the uniaxial behavior. In addition, the decrease in the compressive strength is a function of the lateral strain. The softened stress-strain relationship of ECC is proposed in this paper as shown in Fig. 7. As there is no experimental data of ECC under a biaxial tension condition, the softening effect of reinforced concrete elements derived by Hsu and Mo (2010) is used for ECC in this paper.

As shown in Fig. 7, the compressive stress-strain curve of ECC in a 2-D element subjected to shear exhibits three characteristics. First, the peak point is reduced or ‘softened’ in both strain and stress. Second, the ascending branch is expressed by a bi-linear curve for simplification. Third, similar to concrete, the descending curve is a parabolic curve which intersects the horizontal axis at a large strain of  $4\bar{\epsilon}_{02}$ .

The ascending branch of the softened stress-strain curve of ECC can be simplified as:

$$f_c = E_{ecc} \bar{\epsilon}_c \quad \epsilon_c \leq \zeta \bar{\epsilon}_{01} \tag{8}$$

$$f_c = \zeta \left( f_{ci} + \frac{f_c' - f_{ci}}{\bar{\epsilon}_{02} - \bar{\epsilon}_{01}} (\bar{\epsilon}_c - \bar{\epsilon}_{01}) \right) \quad \zeta \bar{\epsilon}_{01} \leq \epsilon_c \leq \zeta \bar{\epsilon}_{02} \tag{9}$$

The descending branch of the softened stress-strain curve of ECC can be expressed as:

$$f_c = \zeta f'_c \left( 1 - \left( \frac{\bar{\varepsilon}_c / \zeta \bar{\varepsilon}_{02} - 1}{4/\zeta - 1} \right)^2 \right) \quad \varepsilon_c \geq \zeta \bar{\varepsilon}_{02} \quad (10)$$

where  $\bar{\varepsilon}_{02}$  is the strain at peak stress. This value for ECC is usually greater than that for concrete because of a lower Young's modulus. In this paper,  $\bar{\varepsilon}_{02}$  is taken as 0.005 in most of analysis cases.  $\zeta$  is the softened coefficient. Notice that both peak stress  $f'_c$  and the equivalent strain at peak point  $\bar{\varepsilon}_{02}$  are multiplied by  $\zeta$  to achieve the effect of stress softening and strain softening, respectively.  $\bar{\varepsilon}_{01}$  is the strain at the stress  $f_{ci}$ , which is defined as the limit stress for the elastic zone of ECC, and is taken as  $0.8 f'_c / E_{ecc}$ .  $E_{ecc}$  is the initial modulus of ECC, taken as 90 percent of the initial modulus of concrete with the same strength because of the lack of coarse aggregates in ECC mixture design.

#### 4. Seismic behavior of reinforced ECC shear walls

The proposed CSMM-ECC was implemented in the SCS program to perform analyses of the two shear walls SW4 and SW13 described in Section 2. It is assumed that the concrete and ECC have the same compressive strength. The ultimate point in the response curve is defined as the point of 80% of the structure's maximum shear capacity in the descending branch. Some of important aspects of the results obtained from the analyses are discussed to evaluate the effect of ECC in seismic performance of the structures.

##### 4.1 Seismic response of shear walls under monotonic loading

The results as shown in Fig. 8 revealed significant difference between the RC and reinforced ECC shear walls under monotonic loading. Before concrete (or ECC) cracks, ECC shear walls and concrete shear walls have almost identical stiffness. After concrete (or ECC) cracks, the stiffness of each of both shear walls decreases, and the stiffness of ECC shear walls becomes higher than that of concrete walls. The similarity of stiffness before cracking can be explained by two reasons. First, these values of maximum compressive stresses, the tensile stresses at cracking and the tensile strains at cracking are similar. Second, the initial stiffness of the compressive stress-strain curve of ECC is defined to be very close to concrete, i.e. 90% of concrete. The difference of the stiffness between ECC shear walls and concrete shear walls after cracking can be explained by the dissimilarity of the tensile stress-strain curve of ECC and concrete after cracking. After cracking, the tensile stress within concrete decreases and becomes negligible. In contrast, ECC exhibits tensile strain-hardening behavior, which leads to the increased shear capacity of ECC shear walls.

In both cases of SW4 and SW13, the peak strength and ultimate displacements or total drifts of ECC shear walls are greater than concrete shear walls. As shown in Fig. 8a, the peak strength increases about 30% and the displacement increases approximately three times. It is noted that, in the case of SW13, the curve is ductile with the use of concrete and it becomes much more ductile for ECC. In the case of SW4, the behavior of wall which is originally brittle becomes a little ductile when ECC is used, as shown in Fig. 8b. This may result from the ductile behavior of ECC in tension.

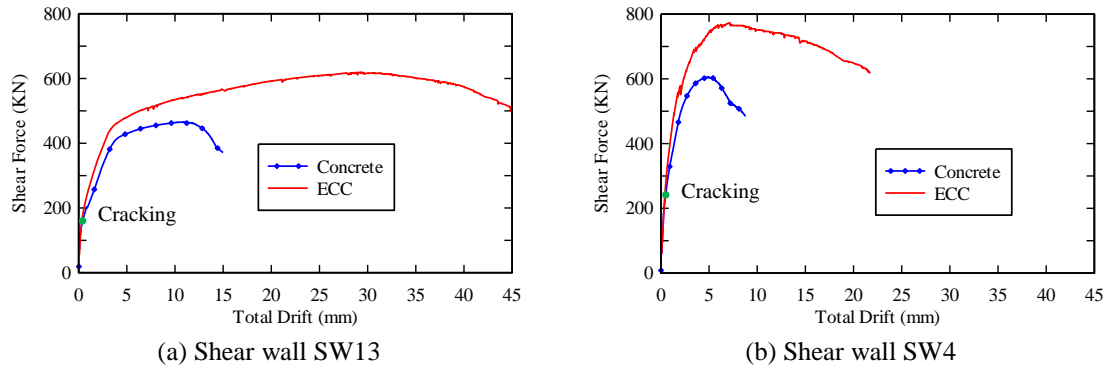


Fig. 8 Seismic responses of shear walls under monotonic loading.

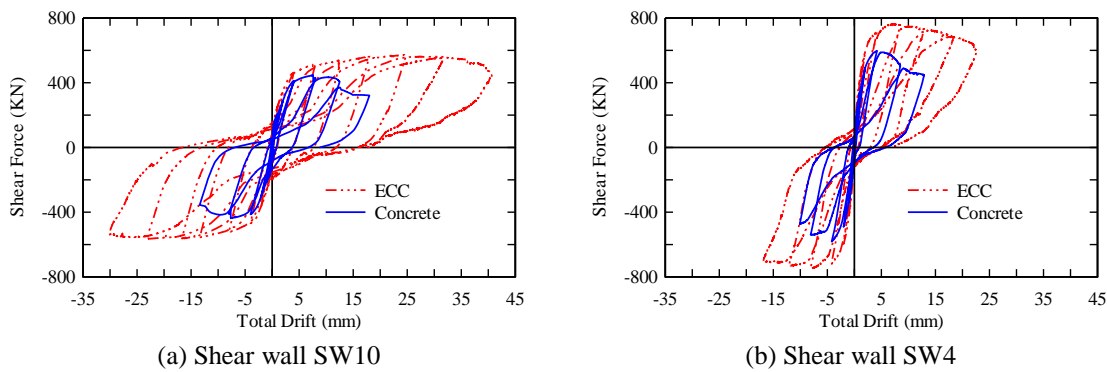


Fig. 9 Seismic responses of shear walls under cyclic loading.

4.2 Seismic response of shear walls under cyclic loading

As reported in Section 2, the CSMM model for RC has been modified for ECC subjected to both monotonic and reversed cyclic loading. The results from the analyses of cyclic loading are presented in Fig. 9. The stiffness, peak strength, and maximum displacement of the shear walls increase significantly similar to the case of monotonic loading. For the sake of the higher ductility, the shear walls can sustain more cycles of loading. Therefore, the energy dissipation capacity is sustainably increased.

4.3 Effect of strain at maximum compressive strength  $\epsilon_o$

Unlike tensile property, not many studies have been done to investigate the compressive property of ECC. The ECC is assumed to have a similar characteristic in compression as confined concrete which is more ductile than normal concrete (Li *et al.* 2006). It is noted from analysis, when the ascending part of the force-displacement curve is affected mostly by the tensile property of material, the descending part is controlled by the compressive property, in that, the strain at peak compressive stress is the dominant parameter.

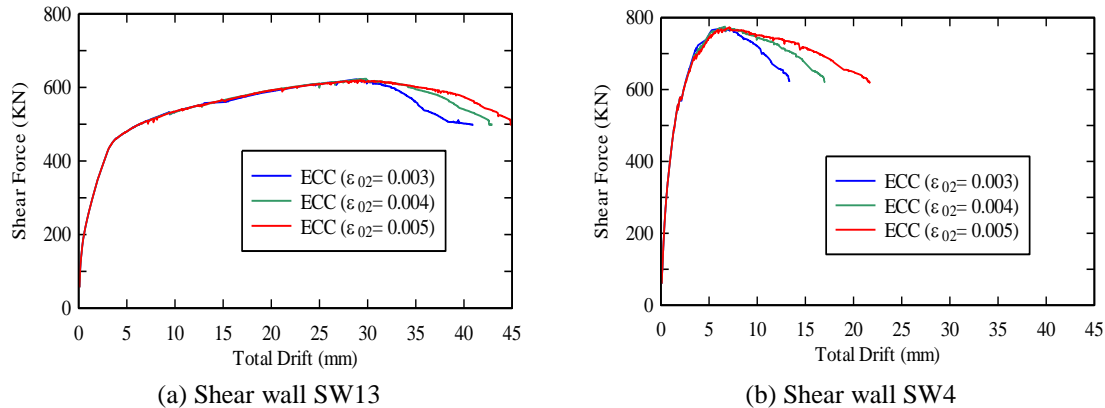


Fig. 3 Seismic responses of shear walls using ECC material with different values of strain at peak strength

Fig. 10 shows the results of the same shear walls using ECC material with different values of compressive strains at peak compressive stress. As the strain at peak compressive stress increases, the stiffness of the descending part increases and the wall fails in a more ductile manner. For the case of ductile shear wall SW13, this change has little contribution in the overall response of the wall. However, this change makes big improvement in the case of SW4 because its original behavior with concrete is brittle. In other words, the ductility of material in compression becomes more important in case of brittle structures and more attention is need.

#### 4.4 Pinching effect

Pinching effect usually occurs in RC structures as a cause of less ductility and reduced energy absorption when the structures are subjected to seismic loading (Favvata and Karayannis 2014). In RC shear walls, the pinching effect is results of steel bar direction deviating from that of the principal stresses. The pinching effect of the RC shear walls will be improved only when rebars are used in the tensile principal stress direction (Mansour and Hsu 2005). Since tensile property of ECC is very ductile, it is expected to enhance the ductility in the tensile principal stress direction. As shown in Fig. 9, the pinching effect of the reinforced ECC shear walls, however, is not much improved compared with RC shear walls. That is because although ECC is more ductile in tension, but the maximum tensile stress is small and the direction of rebars are the same for concrete and ECC, it will not have large influence to help improve the pinching effect on the shear walls.

#### 4.5 Energy dissipation capacity

Fig. 11 shows the difference in term of energy dissipation capacity between concrete and ECC walls analyzed in Sections 4.1 and 4.2. It can be seen that for both analyzed cases of monotonic and cyclic loading, the dissipated energy of ECC shear walls is approximately four times greater than that of concrete shear walls.

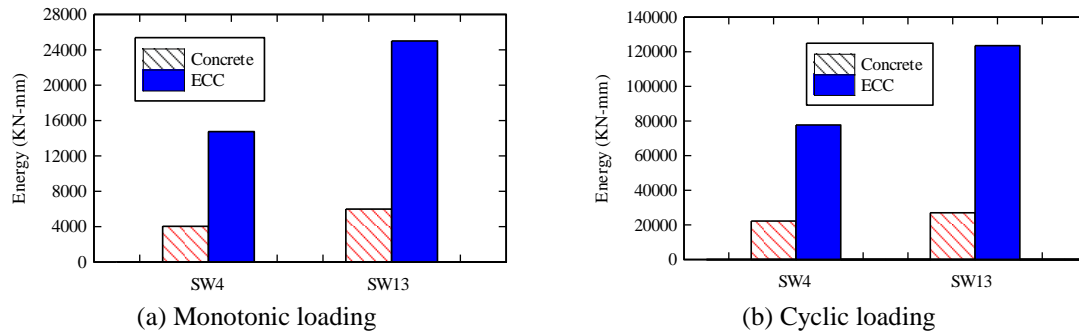


Fig. 11 Comparison of energy dissipation capacity of shear walls using concrete and ECC under monotonic loading and cyclic loading.

## 5. Conclusion

In the paper, the seismic performance of reinforced ECC shear walls was numerically studied. A new Cyclic Softening Membrane Model for ECC was proposed. The seismic response of ECC shear walls under monotonic and cyclic loading, including pinching effect and energy dissipation capacity were examined. It is concluded that reinforced ECC shear walls can improve seismic performance, in terms of load carrying capacity, overall ductility and energy dissipation capacity, when compared with RC shear walls. ECC shear walls can also sustain more cycles than concrete shear walls under cyclic loading. The pinching effect occurred in concrete shear walls still appears in ECC shear walls. In addition, the paper shows that the compression property of ECC also plays an important role in improving the seismic performance of shear walls, especially those with brittle failure.

## Acknowledgment

The research described in this paper is financially supported by U.S. Department of Energy NEUP program (Proj.No. CFP-13-5282). The opinions expressed in this study are those of the authors and do not necessarily reflect the views of the sponsor.

## References

- Favvata, M.J. and Karayannis, C.G. (2014), "Influence of pinching effect of exterior joints on the seismic behavior of RC frames", *Earthq. Struct.*, **6**(1), 89-110.
- Fischer, G. and Li, V.C. (2002), "Effect of matrix ductility on deformation behavior of steel-reinforced ECC flexural members under reversed cyclic loading conditions", *ACI Struct. J.*, **99**(6), 781-790.
- Fischer, G. and Li, V.C. (2003), "Deformation behavior of fiber-reinforced polymer reinforced engineered cementitious composite (ECC) flexural members under reversed cyclic loading conditions", *ACI Struct. J.*, **100**(1), 25-35.
- Gao, X.D. (1999), "Framed shear walls under cyclic loading", Ph.D. Dissertation, University of Houston, Houston.

- Hsu, T.T.C. and Mo, Y.L. (2010), "Unified theory of concrete structures", John Wiley & Sons.
- Kanda, T., Watanabe, S. and Li, V.C. (1998), "Application of pseudo strain hardening cementitious composites to shear resistant structural elements", In Fracture Mechanics of Concrete Structures Proceedings FRAMCOS-3, D-79104 Freiburg, Germany.
- Li, M. and Li, V.C. (2009), "Influence of material ductility on performance of concrete repair", *ACI Mater. J.*, **106**(5), 419-428.
- Li, M. and Li, V.C. (2012), *Rheology, Fiber Dispersion, and Robust Properties of Engineered Cementitious Composites*, In Press, Materials and Structures.
- Li, V.C. (1993), "From micromechanics to structural engineering – the design of cementitious composites for civil engineering applications", *JSCE J. Struct. Mech. Earthq. Eng.*, **10**(2), 37-48.
- Li, V.C. (2002), "Reflections on the research and development of engineered cementitious composites (ECC)", Proceedings of the JCI International Workshop - DFRCC, Takayama, Japan.
- Li, V.C., Lepech, M. and Fischer, G. (2006), "General design assumptions for engineered cementitious composites (ECC)", International RILEM Workshop on High Performance Fiber Reinforced Cementitious Composites in Structural Applications, Honolulu, Hawaii.
- Li, V.C., Mishra, D.K., Naaman, A.E., Wight, J.K., LaFave, J.M., Wu, H.C. and Inada, Y. (1994), "On the shear behavior of engineered cementitious composites", *Adv. Cement Based Mater.*, **1**(3), 142-149
- Li, V.C., Wu, C., Wang, S., Ogawa, A. and Saito, T. (2002), "Interface tailoring for strain-hardening polyvinyl alcohol-engineered cementitious composites (PVA-ECC)", *ACI Mater. J.*, **99**(5), 463-472.
- Mansour, M. and Hsu, T.T.C. (2005), "Behavior of reinforced concrete elements under cyclic shear. II: theoretical model", *J. Struct. Eng., ASCE*, **131**(1), 54-65.
- Mansour, M., Lee, Y.H. and Hsu, T.T.C. (2001), "Cyclic stress-strain curves of concrete and steel bars in membrane elements", *J. Struct. Eng., ASCE*, **127**(12), 1402-1411.
- Mo, Y.L., Zhong, J. and Hsu, T.T.C. (2008), "Seismic simulation of RC wall-type structures", *Eng. Struct.*, **30**(11), 3167-3175.
- OpenSees (2013), "Annual workshop on open system for earthquake engineering simulation", Pacific Earthquake Engineering Research Center, UC Berkeley.
- Ozmen, H.B., Inel, M. and Cayci, B.T. (2013), "Engineering implications of the RC Building Damages after 2011 Van Earthquakes", *Earthq. Struct.*, **5**(3), 297-319.
- Parra-Montesinos, G. and Wight, J.K. (2000), "Seismic response of exterior RC column-to-steel beam Connections", *J. Struct. Eng.*, **106**(10), 1113-1121.
- Yön, B., Sayln, E. and Koksall, T.S. (2013), "Seismic response of buildings during the may 19, 2011 Simav, Turkey Earthquake", *Earthq. Struct.*, **5**(3), 343-357.
- Zhong, J. (2005), "Model-based simulation of reinforced concrete plane stress structures", Ph.D. Dissertation, University of Houston, Houston.
- Zhu, R.R.H. and Hsu, T.T.C. (2002), "Poisson effect in reinforced concrete membrane elements", *ACI Struct. J.*, **99**(5), 631-640.